Application of nanosize polycrystalline SnO_2-WO_3 solid material as CO_2 gas sensor

S. B. Dhannasare[a], S. S. Yawale[b], S.B.Unhale[c], and S.P. Yawale[b]
[a]*Department of Physics, R.L.T College of Science, Akola, India.*
[b]*Department of Physics, Government Vidarbha Institute of Science & Humanities, Amravati-444 604, India.*
[c]*Department of Physics, Arts, Commerce and Science College, Balapur, Akola.*

Recibido el 25 de julio de 2012; aceptado el 17 de agosto de 2012

Among binary metal oxide sensors, tin oxide based sensors have received more attention, due to its high reactivity to many gases. The nanosize SnO_2-WO_3 polycrystalline solid material of different mol% was prepared to form thin films by screen printing method. The sensitivity of the films is measured for different concentration of CO_2 gas at room temperature (303K). The variation of sensitivity with CO_2 gas concentration is found to be linear. The sensor $40SnO_2$-$60WO_3$ shows maximum sensitivity in presence of CO_2 gas. The static and dynamic response of the sensors was studied. The reproducibility and stability for all sensors was good. The average crystallite size was calculated from XRD spectra and found to be of the order of 17.11 to 17.17 nm except pure WO_3 film has 22.91 nm.

Keywords: Tungsten oxide; screen-printing technique; carbon dioxide gas; SnO_2-WO_3; sensitivity.

PACS: 82.47.Rs; 07.07.Df

1. Introduction

Among polluted gases CO_2 is corrosive but plays an important role in greenhouse effect [1]. The metal oxide (MOX) semiconductor sensors have received more attention [2], especially tin oxide based sensors because of its high reactivity to many gases [3]. Addition of WO_3 and La to SnO_2 enhances the sensitivity of SnO_2 to CO_2 gas [5]. The sol gel prepared SnO_2 surface extensively studied using infrared spectroscopy and X-ray by Harrison and Guest [4], reported that crystalline tin (IV) oxide exhibit (110), (101) and (100) planes in ratio 3:1:1 shows more sensitivity to CO_2 gas. Similarly it is also reported that presence of edges and corners influences the creation of hydrogen bond and reactivity of surface species. The resistance of SnO_2 sensor decreases when it is exposed to oxidizing gas CO_2. When SnO_2 is doped with rhodium and cerium oxide alter the electrical properties of SnO_2 by changing semiconducting behavior from n to p type [6]. At lower temperature ($< 150°$C), oxygen adsorbed at SnO_2 surface is mainly in the form of O_2^-. Oxygen ions adsorb on the surface of the film removes electron from the bulk and create a potential barrier that limits electron movement and resistivity [7]. When exposed to an oxidizing gas such as CO_2 then it is chemisorbed on bridging oxygen atoms with the formation of a surface carbonate, subsequently increasing the barrier height and hence resistivity of the sensor. As other metal oxides viz. SnO_2 and TiO_2 etc; WO_3 is also intrinsically n-type bulk semiconductor. The structural arrangement and the surface morphology of the material are main causes to act as sensor hence WO_3 doped gas sensors have specific importance because of structural arrangement of WO_3 [8-10]. It has been reported that the $\alpha SnWO_4$ phase respond to small amount of CO and NO gas [26,27].

It was observed that addition of WO_3 in SnO_2 increases the sensitivity of the sensor when it is exposed to CO_2 gas. Therefore it has been decided to investigate SnO_2-WO_3 solid solution as sensor material for CO_2 gas. Recently the nanoparticle conducting polymers have attracted more attention for exploitation of electrochemical sensors as well as biosensors [11]. One of the authors has investigated polypyrrole as CO_2 gas sensor [12]. The multilayer SnO_2 based CO_2 gas sensor is already studied which gives better response [13] than SnO_2 alone. Also structural changes that occurred in SnO_2-WO_3solid material are studied.

2. Experimental procedure

2.1. Preparation of polycrystalline solid material

The chemicals SnO_2 and WO_3 in powder form (AR grade) were obtained from G. Kuntal & Co. Mumbai. Nine sensors of SnO_2-WO_3 (mol %) were prepared from indigenous powder of respective chemicals. Before mixing of chemicals the powders were calcinated at 800°C and then grinded to fine powder form. After mixing in stiochiometry both powder were heated at 950°C for 4 to 5 h to form nanosize polycrystalline solid material. Then the mixed powder was used for sensor fabrication. The sensors are fabricated on chemically clean and optically plane glass substrate using screen-printing method. The binder for screen–printing was prepared by thoroughly mixing 8-wt % butyl carbitol with 92-wt % of ethyl cellulose. Paste for screen–printing was prepared for each composition by taking powder with sufficient binder in agate mortar and thoroughly mixing it. The paste thus prepared was screen printed on a chemically cleaned glass substrate of size 75×25 mm^2 and then dried at room temperature (303 K) for 24 h. Then all prepared sensors were heated at 373 K for 1 h. During this stage, the volatile organic solvent was removed via decomposition and the print adhered to substrate. For surface resistance measurement the electrodes of

conducting silver paste were formed on adjacent sides of the film and then these films were subjected to heating at 80°C for 15 min for drying the silver paste.

2.2. XRD

The powder of solid solution was characterized by XRD on Philips-1730 (PANalytical) X-ray diffractometer using CuKα radiation (λ=1.5Å) at Vishwesharrayya National Institute of Technology, Nagpur. The diffractogram was in terms of 2θ in the range of 5 to 99°.

2.3. Electrical measurements

The electrical resistance of the film was measured by using voltage drop method adopted by Yawale *et al.*, [14]. The regulated dc voltage 5V was applied to the circuit consisting of standard resistance and sensor in series. A digital microvoltmeter (Scientific equipments, Roorke-India) having resolution $\pm 1\mu$ V and input impedance 10^9 ohm was used for the measurement of voltage across standard resistance.

The gas chamber having dimension $30\times30\times30$ cm^3 with an attached CO_2 gas flow meter (Flowtron make, India) having range 1-10 ml/min was used for keeping the sensors for testing. The gas flow was adjusted to 2 ml/min. The readings were carried out in a CO_2 gas environment at different ppm levels at room temperature (303 K). Experiment was carried out 4-5 times for reproducibility of sensors. Also the stability of the sensors was checked at fixed concentration of CO_2 gas for 4-5 h. No change in the sensor resistance was observed at that concentration and temperature. The thickness of the films was measured by Digimatic outside micrometer (Japan make) having a resolution of ± 1 μm and was in the range of 30 to 34 μm.

The dynamic response of the films was measured by changing the ppm level of the CO_2 gas discontinuously at room temperature.

3. Results and Discussion

3.1. XRD analysis

X-ray diffraction patterns for $20SnO_2$-$80WO_3$, $30SnO_2$-$70WO_3$, $40SnO_2$-$60WO_3$ and pure WO_3 sensors are shown in Fig. 1. The diffractogram is obtained in terms of 2θ and intensity in the range 5–99°. The XRD spectra shows number of peaks suggests the total crystalline behavior of the films. It was investigated that W-O system is rather complex with a large number of phases. From Fig. 1, it is observed that XRD–pattern contain nearly 15-18 peaks, out of these, nearly 14-15 peaks are prominent peaks of WO_3. The tungsten oxide exhibits a cubic perovskite like structure which based on the corners sharing of WO_6 regular octahedral with the W atoms at the centre of each octahedral. The peaks obtained in the range 21-23° corresponds to (002), (200) and (106) phases related to WO_3. Similarly a prominent phase (202) at

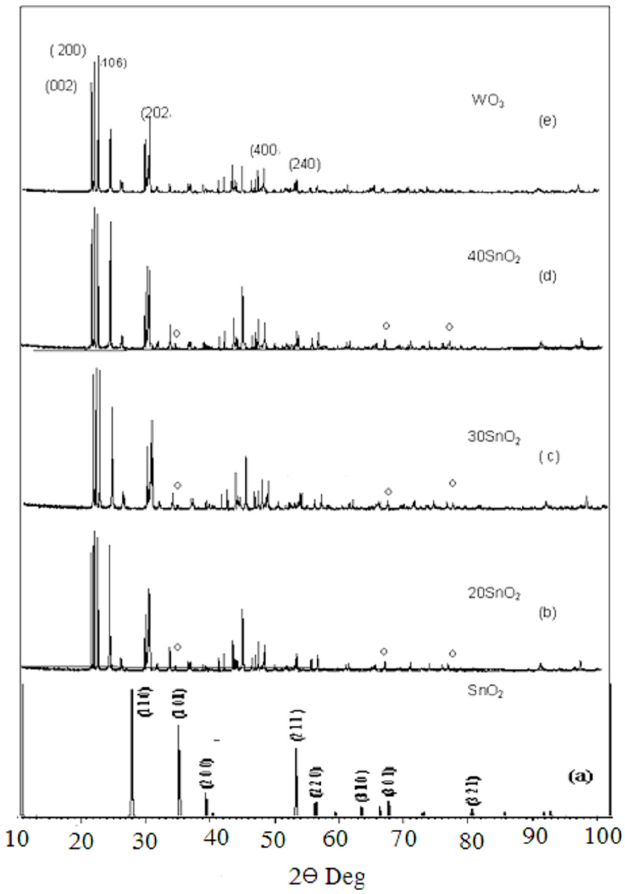

FIGURE 1. XRD pattern of (a) SnO_2 (b) $20SnO_2$-$80WO_3$ (c) $30SnO_2$-$70WO_3$ (d) $40SnO_2$-60 WO_3 (e) WO_3.

about 30° is observed in all samples corresponds to WO_3. In WO_3 five distinct crystallographic modifications takes place between absolute zero and its melting point (1700 K).When temperature is decreased from the melting point, the crystallographic modifications: tetragonal-orthorhombic-monoclinic-triclinic-monoclinic having phases αWO_3, βWO_3, γWO_3, δWO_3 and sWO_3 respectively forms [15-20]. The observed peaks of SnO_2 having (h,k,l) values (101), (301) and (321) are reflected in all samples and related to the stable state of cassiterite or rutile phase. The lattice parameter values obtained for SnO_2 are a=b= 4.7382 Å and c=3.1771Å with c/a ratio of 0.6725. These values are in close agreement with the values reported by Diegnez [21] and Robertson [22,23]. It has been reported that thin films of SnO_2-WO_3 mixed oxides crystallize in the tetragonal, cassiterite SnO_2 structure with the lattice parameters slightly larger than those for undoped SnO_2. This is in agreement with the ionic radii of W^{6+} (0.074 nm) and Sn^{4+} (0.071 nm). This suggests the substitutional mechanism of W incorporation. The influence of the substrate temperature during film deposition manifests itself as a systematic change of the preferred orientation in the structure from (101) at 100°C to (110) at 400°C accompanied by the progressive film crystallization [28].

The average grain size can be determined from XRD pattern using Debye-Schrrer formula [24]

$$D = K\lambda/\cos\theta. \quad (1)$$

Where D is the crystallite size, K is the shape factor, which can be assigned a value of 0.89 if shape is unknown, θ is the diffraction angle at maximum peak intensity, λ is the wavelength of radiation and ß is the full width at half maximum of diffraction angle in radians. The average crystallite size for these samples is found to be in the range of 17.17 to 17.11 nm. It is observed that the average crystallite size is found to be nearly same for all samples except pure WO_3 sample for which it is 22.91 nm. This indicates that the crystallite size of SnO_2-WO_3 composite decreases.

3.2. Sensitivity of sensors

The resistance of the prepared sensors is found to increase with increasing the CO_2 gas concentration. The sensitivity of the sensor is calculated by the following formula

$$S = (R_g - R_a)/Ra = \Delta R/R_a. \quad (2)$$

Where R_a is the resistance of the sensor in air and R_g is the resistance of the sensor in CO_2 gas.

The sensitivity of these sensors increases linearly with the CO_2 gas concentration at room temperature (303 K). The variation of sensitivity with CO_2 gas concentration at room temperature for various concentration of SnO_2 is shown in Fig. 2. It is observed that the sensor 40SnO_2-60WO_3 shows highest sensitivity while sensor of pure SnO_2 shows least sensitivity to CO_2 gas. The sensor 40SnO_2-60WO_3 exhibits linear dependence on CO_2 gas concentration up to 1100 ppm, and then it reaches to a saturation level while the sensor of pure SnO_2 and 80SnO_2-20WO_3 shows linear dependence up to 800 ppm. With a fixed surface area, lower gas concentration implies a lower coverage of gas molecules on the surface. An increase in the gas concentration raises the surface coverage eventually leading to saturation level, which determine upper limit of detection. A plot of sensitivity versus WO_3 composition at three different concentration of CO_2 gas (100, 200 and 300 ppm) is shown in Fig. 3. The overall behavior at three different concentration of CO_2 is same. It was found that the sensor 40SnO_2-60WO_3 has highest sensitivity than rest of the sensors. Thus by adding an increasing amount of WO_3 to SnO_2 sensitivity of corresponding sensor increases up to 40SnO_2-60 WO_3 sensor which has maximum sensitivity, thereafter sensitivity decreases and remain constant by addition of further amount of WO_3. It was investigated that pure SnO_2 has poor response to CO_2 gas as compared to WO_3 added sensors, but when doped with WO_3 create several defects in the structure of SnO_2 which enhances electronic density on metallic W at adjacent cations and hence WO_3 acquire semiconducting property. Moreover addition of WO_3 to the SnO_2 creates rough surface and makes more surface area. In case of 40SnO_2-60WO_3 sensor the active

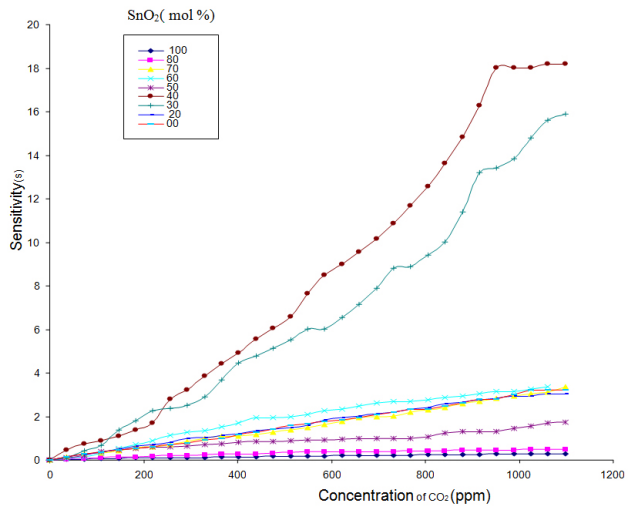

FIGURE 2. Variation of sensitivity with concentration of CO_2 (ppm) gas at room temperature (303K).

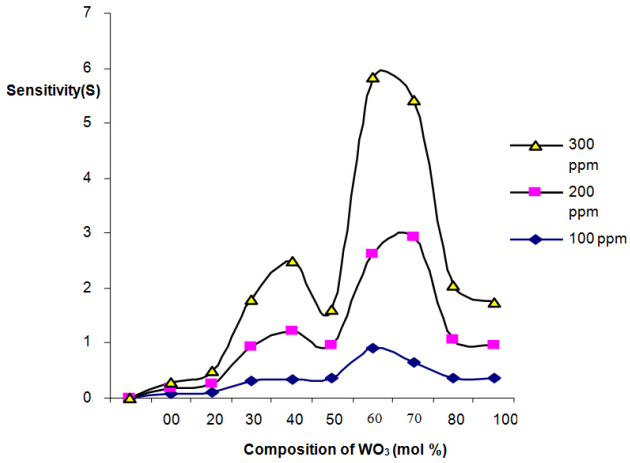

FIGURE 3. Variation of sensitivity with WO_3 composition at room temperature for 100, 200 and 300 ppm of CO_2 gas.

surface area will be more than the other samples causing more adsorption of gas therefore the sensitivity will be more.

As far as the gas sensing is concerned the structural properties are utmost important. The electrical and optical properties of tungsten trioxide are dependent on the crystalline structure. The worth mentioning point is that the tungsten trioxide structure is likely to host several kinds of defects. The most common is the lattice oxygen vacancy where an oxygen atom is absent from a normal lattice site. This causes to increase an electronic density on the metallic W adjacent cations leading to the formation of donor like state slightly below the edge of the conduction band of the oxide. Because of this defect the crack develop along the 100 crystallographic plane due to which the surface of the tungsten oxide changes, in such a situation the half of the tungsten atoms remain in the valence states 6 and are connected to the terminal oxygen ions giving one of the electron to nearest tungsten ion which transforms into W^{5-} state [25]. Another possibility is that all tungsten atoms at the surface change their valence

TABLE I. Composition, Resistance change per ppm, Response time and Recovery time of sensors

Sr. No	Sensors	Composition (mol %) SnO_2-WO_3	Change in Resistance per ppm (MΩ)	Response time (s)	Recovery time (s)
1	A	100-00	25.0	180	62
2	B	80-20	401.7	122	113
3	C	70-30	1894.7	132	137
4	D	60-40	579.0	120	92
5	E	50-50	1022.7	132	53
6	F	40-60	14270.5	127	42
7	G	30-70	2023.5	232	53
8	H	20-80	727.2	123	105
9	I	00-100	1334.7	180	46

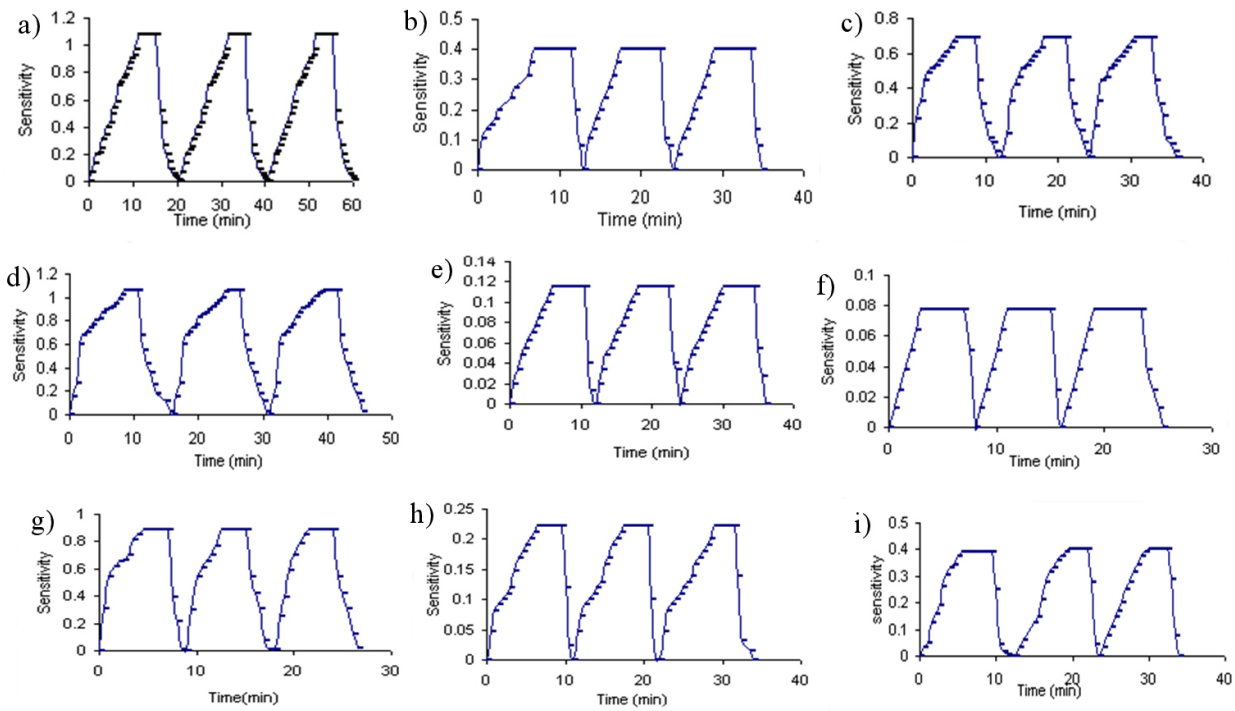

FIGURE 4. Step response of the sensors at room temperature (303 K) for 100 ppm of CO_2 gas concentration.

state to 5 to form a surface by $W^{5-}O_2$ terminal layer. This surface W^{5-} site reacts with the oxidizing atmosphere leading to the adsorption of the gas molecules. Neither only the tungsten oxide is important but also the tin oxide is equally important as far as gas sensing is concerned. In the solid solution of SnO_2-WO_3 the roughness of the surface and the active surface area enhance the sensitivity.

3.3. Static and dynamic response

The response time is defined as the time taken to reach 90% of the response when ppm of gas is changed. The time taken to reach 90% of recovery when gas is turned off is known as recovery time. The static response of prepared sensors is studied at 100 ppm of CO_2 gas at room temperature (Fig. 4). On and off response time is calculated from the steps. The resistance change per ppm is also calculated which is reported in Table I. From Table I, it is observed that change in resistance per ppm of CO_2 gas is large for sensor $40SnO_2$-$60WO_3$ which is highly sensitive and minimum for pure SnO_2 sensor which is least sensitive and this can also be verified from Fig. 2.

The dynamic response of the sensors for 100, 200 and 300 ppm of CO_2 gas concentration at room temperature (303 K) is shown in Fig. 5. The sensor is exposed to CO_2

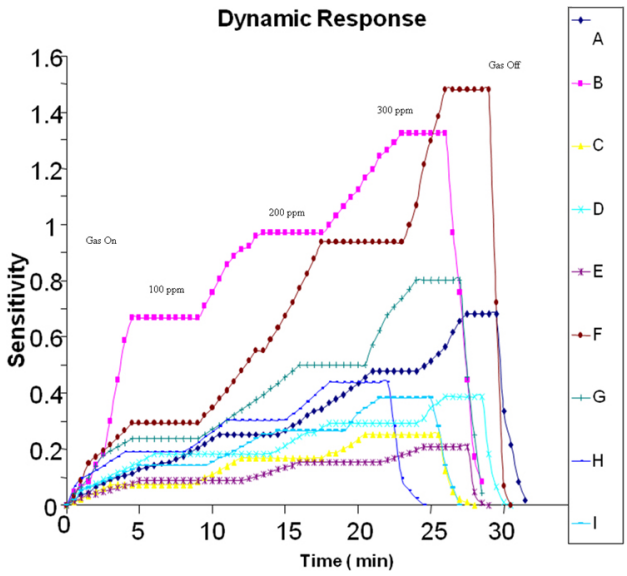

FIGURE 5. Dynamic response of sensors at 100, 200 and 300 ppm of CO_2 gas concentration.

gas with a step of 100, 200 and 300 ppm and then suddenly exposed to air. The time dependent resistance changes were recorded till the original value of resistance reaches. The response and recovery time are two important parameters to characterize a sensor. From Table I it is observed that sensor $40SnO_2$-$60WO_3$ that is highly sensitive takes response time 142 s and recovery time as 42 s. It has been reported that the SnO_2-TiO_2 sensors' response and recovery time in H_2 sensing is 20 min and 5-6 min respectively [29].

3.4. Stability of sensors

The sensors under study were nearly stable even after 41 h. The sensor $40SnO_2$-$60WO_3$ shows maximum stability amongst rest of the sensors. From Table I it is seen that as concentration of WO_3 increases, sensor acquires more stability. When such sensors expose to an oxidizing gas like CO_2, then it is chemisorbed on bridging oxygen atoms with formation of a surface carbonate, subsequently increasing the barrier height and the resistivity [7].

3.5. Repeatability

For studying the repeatability, each sensor was exposed to CO_2 gas environment at 100 ppm for 15 min and changes in resistance were recorded. After refreshing, further two cycles were repeated. Thus each sensor was repeated for three times. Repeatability of sensors was simultaneously observed during study of step response. It was observed that each sensor exhibited good repeatability, except sensor of pure WO_3 where there is slight irregularity in second cycle, but third cycle is again replica of second.

4. Conclusion

These sensors with different mol % of SnO_2 and WO_3 prepared by screen–printing technique were used to investigate for the CO_2 gas sensing properties. The studied sensors show linear variation of sensitivity with CO_2 gas ppm. The sensor $40SnO_2$-$60WO_3$ shows highest sensitivity. The response time for these sensors lies between 2.5 to 5.5 min while all other sensors recover themselves within duration of 1 to 2.5 min. XRD study reveals that these sensors have polycrystalline nature. The resistance change per ppm of CO_2 gas concentration at room temperature is more for $40SnO_2$-60 WO_3 sensor and minimum for pure SnO_2 sensor. The response time for these sensors lies between 180 to 232 s. Similarly recovery time for them lies between 42 to 137 s, thus these sensors exhibit good recovery time compared to their response time. These sensors possess better stability and it will not change even after a time span of 41 h. Similarly every sensor exhibit better reproducibility.

Acknowledgments

Authors are thankful to Head, Department of Physics and Director, Government Vidarbha Institute of Science and Humanities, Amravati for providing laboratory facilities and G.K. Reddy, Technical Officer, Instrument Maintenance Facility of the same institute for meticulous corrections in the graphs and manuscript.

1. M. Estis, G. Volpe, L. Massignan, and G.Palleschi, *J. Agric. Food Chemistry* **46** (1998) 4233-4237.
2. N. Taguichi, *Gas sensor studies on sensor film deposition* (1970) 1280809.
3. S. Supothina, *Gas sensing properties of nano-crystalline SnO_2 thin films prepared by liquid flow deposition Sensors and Actuators B* **93** (2003) 526-530.
4. P.G. Harrison, A. Guest, *J. Chem Soc* **83** (1987) 3383.
5. A. Marsal, A. Cornet, J.R. Morante, *Sensors and Actuators B* **94** (2003) 324 -329.
6. H. Teteysz, D. Nisch, L.J. Golanka, *Sensors and Actuators B* **47** (1998) 153-157.
7. M. Batzill and U. Diebold, *Progress in Surface Science* **79** (2005) 47-154.
8. S.V. Gopal Reddy, W. Cao, O.K. Tan, W. Zhu, S.A. Akbar, *Sensors and Actuators B* **94** (2003) 99.
9. B. Podor, Zs. J. Horvath, P. Basa; *Semiconductor Nanocrystals* **1** (2005) 123; Budapest, Hungary.
10. S.P. Yawale, S.S. Yawale, G.T. Lamdhade, *Tin oxide and zinc oxide based doped humidity sensors Sensors and Actuators A* **135** (2007) 388-393.
11. A. Morrin, K. Crowley, E. Kazimieraska, X. Luo, M.R.Smyth, G.G. Wallance, A.J. Killard, *Elecrtoactive polymers:Materials*

and devices Vol. 3 pp 83 Eds. (S.A. Hashmi, Amita Chandra and Amreesh Chandra, Mc-Millan Pub. New Delhi 2009).

12. S. A. Waghuley, S. M. Yenorkar, S. S. Yawale, S. P. Yawale, *Sensors and Actuators B* **128** (2008) 366-373.
13. S. A. Waghuley, S. M. Yenorkar, S. S. Yawale, S. P. Yawale, *Sensors and Transducers* **79** (2007) 1180-1185.
14. S.P. Yawale, S.V. Pakade, *J. Mater. Sci. (UK)* **28** (1993) 5451-5455.
15. W. Kehl, R. Hay, D. Wahl, *J. Appl. Phys* **23** (1952) 212-215.
16. E. Saljie, *Acta Crystallogr. B* **33** (1977) 547-577.
17. S. Tanisaki, *J. Phys. Soc. Jpn* **15** (1960) 573-581.
18. B.U. Loopstra, J.L. Rietveld, *Acta Crystallogr. B* **25** (1969) 1420-1421.
19. R.Diehl,G.Brandt,E.Saljie; The crystal structure of triclinic WO_3;Acta Crystallogr. B34(1978) 1105-1111.
20. E. Saljie *Ferroelectrics* **12** (1976) 215-217.
21. A. Dieguez, *Structural analysis for the improvement of SnO_2 based gas sensor* Ph.D. Thesis, (Universitat de Barcelona, Barcelona, 1999).
22. J. Robertson, *Phys.Rev.B* **30** (1984) 3520-3522.
23. JCPDS data file no.41-1445(1997).
24. B.D.Cullity, *Elements of X-ray diffraction* (Addison–Wesley Pub. Co. Inc., London, 1978).
25. A. Kuzmin, J. Purans, E. Czzanelli, C. Vinegoni, G. Mariotto, *J Appl. Phys.* **84** (1998) 5515-5524.
26. J.L. Solis, V. Lantto, *Sensors Actuators B* **24** (1995) 591.
27. J.L. Solis, V. Lantto, *Physica Scripta T* **69** (1997) 281.
28. M. Radecka, P. Pasierb, K. Zakrzewska, A. Kowal, *Electron Technol* **33** (2000) 73.
29. M. Radecka, K. Zakrzewska , M. Re, kas, *SnO_2–TiO_2 solid solutions for gas sensors Sensors and Actuators B* **47** (1998) 194-204.